International Journal of Multiphase Flow 191 (2025) 105312

Contents lists available at ScienceDirect

International Journal of Multiphase Flow

journal homepage: www.elsevier.com/locate/ijmulflow

Research Paper

A semi-analytical description of the flow of unidirectional, collisional suspensions via extended kinetic theory

Diego Berzi [a], Ashkan Pilbala [b], Luigi Fraccarollo [c,*]

[a] Department of Civil and Environmental Engineering, Politecnico di Milano, Milano 20133, Italy
[b] Department of Civil, Environmental and Architectural Engineering, Università degli Studi di Padova, Padova, 35131, Italy
[c] Department of Civil, Environmental and Mechanical Engineering, Università degli Studi di Trento, Trento, 38123, Italy

ARTICLE INFO

Keywords:
Intense sediment transport
Collisional suspension
Extended kinetic theory

ABSTRACT

We address the collisional transport of cohesionless sediments over a particle bed driven by a gravitational turbulent stream under steady and fully developed flow conditions. The sediment-laden flow forms self-equilibrated resistance mechanisms at the bed surface, below which the sediments are at rest. The principle of mass, momentum, and energy conservation, for both the fluid and the particle phases, gives rise to a challenging set of differential equations, demanding closures for stresses, interaction forces and exchange of energy among the phases and energy dissipation in particle–particle encounters. We introduce a semi-analytical solution of steady, unidirectional collisional suspensions in the framework of the kinetic theory of granular gases, extended to deal with a high volumetric concentration of frictional, nonspherical sediments and the influence of the fluid drag in between collisions. We supplement the extended kinetic theory with a single-parameter and depth-adaptive, although arbitrary, concentration profile. Then, the set of nonlinear differential equations can be solved in a straightforward fashion. As part of the analytical procedure, the concentration parameter is determined without data fitting. The agreement with laboratory experiments performed with mixtures of plastic cylinders in water, in a range of strength of the turbulent shearing fluid and angle of inclination of the flow, is remarkable in terms of profiles of particle mean velocity, velocity fluctuations, and concentration, at least in the part of the flow where the length of the particle trajectories in between successive collisions can be considered unaffected by gravity and buoyancy.

1. Introduction

The topic of sediment transport has a long history of research and a variety of nomenclatures has been introduced to describe, even partially, its vast phenomenology, with special emphasis on the characteristics of the motion of the solid particles carried by, at least on Earth, either air or water. Bedload (Meyer-Peter and Müller, 1948; van Rijn, 1984), saltation (Bagnold, 1941), sheet flow (Jenkins and Hanes, 1998; Gao, 2008; Gonzalez-Ondina et al., 2018), and suspension load (Rouse, 1939) have been and are still used to define various types of sediment transport, often with partial super-positions and ambiguity. Part of the issue is that sediment transport involves a distribution of sizes of the solid particles, and sizes matter when, e.g., comparing the forces acting on the grains. Hence, different regimes of sediment transport usually coexist. To complicate the physical understanding and the mathematical modelling of the phenomenon, real flows are often affected by complex geometries of the boundaries and undergo transients.

To clean up the field, let us focus on an assembly of particles, well-sorted in all aspects (size, shape, density, etc.), transported by a shearing, turbulent fluid over a basal boundary that does not move. The latter can be a rigid bottom or comprise a loose packing of not moving or barely moving (Komatsu et al., 2001) particles identical to those flowing above it. We refer to these two scenarios as sediment transport over rigid or erodible beds, respectively. Then, bedload, in its original spirit (Meyer-Peter and Müller, 1948), is the regime of sediment transport in which only a few particles are moving, and these particles leave the bed at a certain instant, fly over the bed under the effect of gravity and fluid forces, and eventually retouch the bed at the end of their solitary flights. Here, they may rebound or stop. Occasionally, there might be a few mid-fluid collisions above the bed, but their effect on the transport rate is negligible. We might also call bedload as the ballistic regime. In the field of windblown sand, this ballistic regime is called saltation (Sauermann et al., 2001; Andreotti,

* Corresponding author.
E-mail address: luigi.fraccarollo@unitn.it (L. Fraccarollo).

https://doi.org/10.1016/j.ijmultiphaseflow.2025.105312
Received 8 November 2024; Received in revised form 11 May 2025; Accepted 31 May 2025
Available online 25 June 2025

2004; Valance et al., 2015), and represents the main mode of sediment transport.

On the other side of the spectrum, suspension is the regime of sediment transport in which particles can fly over the bed without directly interacting with the bed itself. For this to happen, we must look for physical mechanisms able to provide one or more forces that balance the buoyant weight of the particles. This physical mechanism can be either the momentum exchange in interparticle collisions or the turbulent lift generated by the interstitial fluid. We can thus distinguish between collisional and turbulent suspensions.

Next, quantitative criteria must be provided to identify the above-mentioned regimes. By increasing the intensity of the shearing flow, the ballistic regime gives way to the collisional suspended regime (Ralaiarisoa et al., 2020). The length of the particle trajectories comprised between two successive interactions with the bed or other particles can be suitably employed to distinguish between these regimes. Indeed, there is a maximum length, called the mean free path in the literature of kinetic theory (Chapman and Cowling, 1970), for which the influence of the external forces acting on the particles, such as gravity, buoyancy and drag, can be safely ignored when calculating the stresses originated from the collisional exchange of momentum in the particle phase of the mixture (treated as a continuum). The transition from ballistic to collisional sediment transport takes place when the averaged trajectory length equals the mean free path (Pasini and Jenkins, 2005). Given that the mean free path is a decreasing function of the particle concentration (Chapman and Cowling, 1970), there is a minimum concentration above which the regime is collisional. In the collisional regime, the constitutive relations of the kinetic theory of granular gases can be employed (Jenkins and Savage, 1983; Garzó and Dufty, 1999).

If the intensity of the turbulence is large enough to overcome the particle buoyant weight, the sediment transport enters the turbulent suspension regime. Given that, in a fluid at rest, the competition between gravity, buoyancy and drag determines the particle settling velocity, and that a good measure of the turbulence intensity is given by the fluid shear velocity (the square root of the fluid shear stress over the fluid mass density), the ratio of the fluid shear velocity over the particle settling velocity, which is inversely proportional to the Rouse number (Rouse, 1939), has been proposed as a criterion for the onset of turbulent suspensions. There is a critical value of this ratio above which the turbulent suspension regime takes over (Pugh and Wilson, 1999).

Even in the idealized case of sediment transport of mono-sized particles and steady, uniform flow, the concentration and the fluid shear velocity are local fields, heterogeneous in the flow domain. As such, the ballistic, collisional and turbulent suspension regimes can be simultaneously present in different regions of the spatial domain, perhaps in a stratified fashion. There might even be regions of the flow where two or more of the regimes mentioned above coexist. Models of sediment transport stratified into a purely collisional and a turbulent-collisional layer have been proposed (Berzi and Fraccarollo, 2016). On the other hand, the existence of a region in which both ballistic and collisional mechanisms conspire to determine the particle stresses has recently been dealt with (Chassagne et al., 2023). We deem it will be crucial to widen our understanding of the role of gravity and fluid interactions on inter-particle collisions, and also the transition from saltation (like in ordinary bed load) to collisional suspensions (Ralaiarisoa et al., 2020).

In this work, we focus on the model of sediment transport over erodible beds in the collisional regime, particularly on the transport of solid particles in water in inclined channels, for which detailed measurements of the distributions of particle volumetric concentration, particle mean velocity and velocity fluctuations are available (Capart and Fraccarollo, 2011), allowing for a severe test of continuum models. Co-authors of the present paper have already used the kinetic theory of granular gases in attempts to solve this regime of sediment transport (Berzi, 2011; Berzi and Fraccarollo, 2013, 2016). In so doing, they have formulated a system of differential equations governing the motion of the two phases, solid particles and liquid, but were unable to find full numerical solutions of the system. They have provided approximate analytical solutions by stratifying the flow domain into a few layers characterized by different physical mechanisms and integrating the differential equations through simple trapezoidal rules.

Complications of solving balance equations with closures from the kinetic theory of granular gases come from the fact that the particle phase must be treated as compressible, and the equation of state, the granular viscosity and pseudo-thermal conductivity, and the collisional dissipation rate of fluctuation energy are all strongly nonlinear functions of the particle concentration. Chassagne et al. (2023) have recently proposed a two-phase continuum model for collisional suspensions based on the kinetic theory of granular gases that includes the presence of both saltating particles and a Coulomb-like frictional behaviour of the solid phase near the bed. They were able to numerically integrate the differential equations and to make comparisons against coupled fluid-discrete element simulations of spheres. When applied to physical experiments (Ni and Capart, 2018), however, their model seems to strongly underpredict the intensity of particle agitation.

Here, we introduce a strong simplification by uncoupling the determination of the particle concentration from the other hydrodynamic variables. First, we assume that the concentration distribution in the flow is such that it maximizes some definition of the Shannon entropy (Lien and Tsai, 2003). This permits, then, to solve analytically the momentum and energy balances, with the constitutive relations of the kinetic theory of granular gases, extended to include the role of particle friction (Jenkins and Zhang, 2002; Berzi and Vescovi, 2015), velocity correlation (Jenkins, 2007; Jenkins and Berzi, 2010), fluid drag (Jenkins et al., 2010), particle softness (Berzi and Jenkins, 2015), and cylindrical shape (Berzi et al., 2022). We also include the role of the particles in modulating the fluid turbulence (Berzi and Fraccarollo, 2015; Gonzalez-Ondina et al., 2018) and the mutual influence of the turbulent fluctuations and the particle agitation (Hsu et al., 2004; Berzi and Fraccarollo, 2015). We limit the analysis to the region of the flow dominated by collisions, but, through comparisons with experiments of plastic cylinders in water (Capart and Fraccarollo, 2011), we confirm, as suggested in Chassagne et al. (2023), that the ballistic regime, and/or a combination of the ballistic and collisional regime, are indeed crucial in the case of sediment transport in water.

The paper is organized as follows: we introduce the governing equations and show how to solve them in Section 2. In Section 3, we make comparisons between the predictions of the theory and the experimental results on the sediment transport of plastic cylinders and gravel in water. Finally, the paper ends with concluding remarks in Section 4.

2. Theory and solution development

The sketch of the flow configuration is depicted in Fig. 1. We focus on the steady, fully developed, free-surface flow of a mixture of a liquid, of mass density ρ and molecular dynamic viscosity η, and identical, inelastic spheres, of diameter d and mass density ρ_p, over an erodible bed composed of the same particles, assumed at rest. Particles are driven into collisions by the combined effect of gravity and the drag exerted by the turbulent liquid. We characterize the collisions through the coefficients of normal, e_n, and tangential restitution, e_t, i.e., the negative ratio of pre- to post-collisional relative velocities normal and tangential to the plane of contact; the coefficient of sliding friction, μ; and the effective coefficient of restitution, ε, which is a function of e_n, e_t and μ, and accounts for the role of friction in the rate at which energy is dissipated in collisions (Jenkins and Zhang, 2002; Larcher and Jenkins, 2013).

We limit the analysis to situations in which the thickness of the transport layer, h, is, at least, a few particle diameters. We assume that the momentum exchange in collisions is at the origin of the dominant

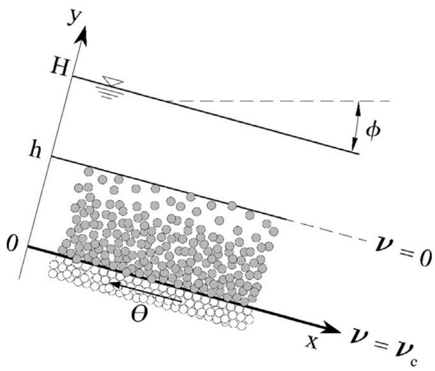

Fig. 1. Sketch of the flow configuration with the frame of reference and concentration reference values at specific positions.

stresses in the particles. We will provide a criterion to distinguish between a lower collisional-dominated region and, above it, a region where the particles follow trajectories with ballistic features. On top of the transport layer there is a turbulent liquid layer, and the total thickness of the transport and liquid layer over the erodible bed is H. The range of validity of the assumption mentioned above of a collisional-dominated regime is given in Berzi and Fraccarollo (2013, 2016) as a region in the phase diagram with the Shields number Θ, the dimensionless strength of the shearing flows, on one axis and the angle of inclination of the bed, ϕ, on the other. We limit the analysis to flows for which the turbulent lift on the particles is weaker than the particle buoyant weight.

We take x and y to be the direction parallel and perpendicular to the erodible bed, respectively, and neglect variations in the spanwise direction. The surface of the bed is located at $y = 0$. The local particle velocity and concentration are u and ν, respectively. In what follows, all quantities are made dimensionless using the particle density and diameter, and the reduced gravitational acceleration, $g(\sigma - 1)/\sigma$, where g is the gravitational acceleration and $\sigma = \rho_p/\rho$ is the density ratio. With this, the inverse of the dimensionless molecular viscosity of the liquid is σR, with $\mathrm{R} = \rho d\sqrt{gd(\sigma-1)/\sigma}/\eta$ being the fall particle Reynolds number.

We obtain a semi-analytical solution of the flow through the sequential steps described in the following, assuming that the 4 control parameters of the problem, i.e., σ, R, ϕ and Θ are known.

2.1. The choice of an analytical concentration profile based on a single parameter and depth-adaptive

An appropriate analytical expression for the concentration profile in the sediment layer must satisfy the conditions of: being monotonic, comprised between a minimum and a maximum; allowing for changing concavity, according to, e.g., the intensity of the shearing; and containing as few free parameters as possible.

The minimum and maximum concentrations correspond to the values of the concentration at the top of the sediment layer and at the surface of the erodible bed, respectively.

Here, we simply take the minimum value to be zero. As shown in Berzi et al. (2019, 2020), the interface between the flow and the erodible bed is characterized by a critical value of the particle concentration, ν_c, which, for spheres, is solely dependent on the sliding friction coefficient. For cylinders, the critical concentration depends on the sliding friction and the aspect ratio (Berzi et al., 2022). The critical concentration is the minimum value of ν at which rate-independent components of the stresses first develop (Chialvo et al., 2012).

The concentration profile given in Lien and Tsai (2003), where the Shannon maximum entropy principle (Shannon, 1948) was exploited,

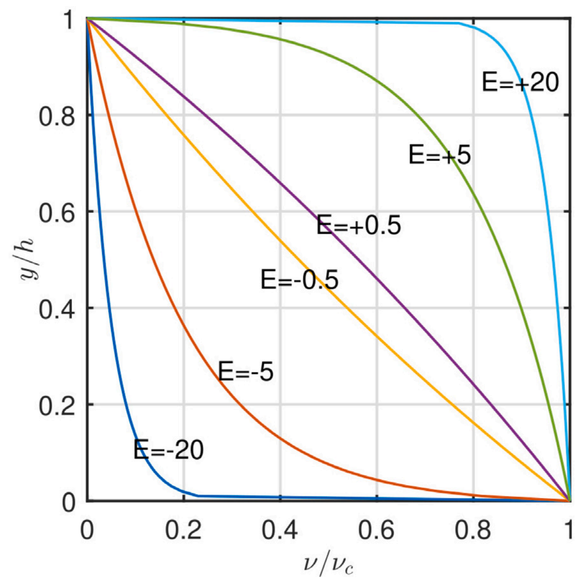

Fig. 2. Entropic concentration profiles from Eq. (1) for different values of the entropic parameter.

is a single-parameter distribution which satisfies our requirements and reads

$$\nu = \frac{\nu_c}{E} \ln\left[\exp E + (1 - \exp E)\frac{y}{h}\right], \tag{1}$$

where E is an arbitrary dimensionless constant, defined as the entropic parameter.

Fig. 2 shows how the concentration profile changes as a function of E, in the range between −20 and 20. Negative or positive values of E give concave or convex concentration profiles, respectively. With E close to zero (but different from zero, as $E = 0$ would make Eq. (1) singular), the concentration profile is approximately linear.

The average concentration in the transport layer can then be determined by integrating Eq. (1),

$$\bar{\nu} = \frac{1}{h}\int_0^h \nu\, dy = -\nu_c\left(\frac{1}{E} + \frac{\exp E}{1 - \exp E}\right). \tag{2}$$

2.2. Determination of the depth, h, of the transport layer

We first assume that the particle shear stress, s, is at yield at the bed, that is $s(y = 0) = s_0 = k_0 p_0$, where the yielding coefficient k_0 is taken to be the ratio of the particle shear stress over the particle pressure when the concentration is equal to ν_c (Berzi and Vescovi, 2015). p_0 is the granular pressure at the surface of the bed ($y = 0$), which equals the normal projection of the buoyant weight of the solid component of the flow mixture:

$$p_0 = \bar{\nu} h \cos\phi. \tag{3}$$

The expression of k_0, as a function of e_n, ε and ν_c, is (Berzi, 2024)

$$k_0 = \left[\frac{24 J_\infty\left(1-\varepsilon^2\right)}{5\pi\left(1+e_n\right)^2}\right]^{1/2}\left[1 + \frac{26(1-\varepsilon)}{15}\frac{\nu_c - 0.49}{\nu_{rcp} - \nu_c}\right]^{-1/2}, \tag{4}$$

where ν_{rcp} is the concentration at random close packing (the maximum concentration for a random assembly of frictionless particles, equal to 0.64 for spheres (Torquato, 1995)), and

$$J_\infty = \left[\frac{1+e_n}{2} + \frac{\pi}{4}\frac{\left(1+e_n\right)^2\left(3e_n - 1\right)}{24 - 6\left(1-e_n\right)^2 - 5\left(1-e_n^2\right)}\right]\left(1 + \frac{\pi}{12}\frac{3e_n - 1}{3 - e_n}\right). \tag{5}$$

Then, we define the Shields number, Θ, as the dimensionless total shear stress of the mixture at the surface of the bed. The Shields number

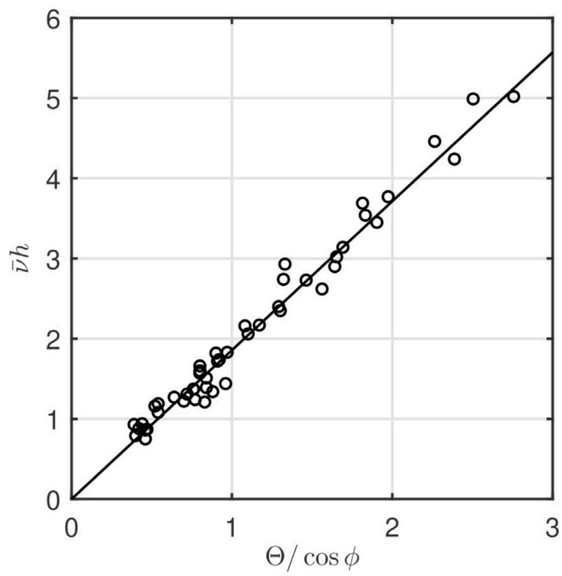

Fig. 3. Measured (symbols, after Capart and Fraccarollo (2011)) and predicted (line, from Eq. (6), with $k_0 = 0.38, \sigma = 1.51$ and $\nu_c = 0.61$, as appropriate for plastic cylinders in water) mass hold-up against $\Theta/\cos\phi$.

quantifies the intensity of the shearing flows, and we take it as an input of the problem. At large concentrations, the fluid turbulence is heavily suppressed, but the velocity fluctuations of the particles induce a shear stress in the fluid proportional, through a function of the concentration, to the shear stress of the particles (Berzi and Fraccarollo, 2015). Hence, $s_0 + S_0 = \Theta$, being S_0 the shear stress of the liquid phase at $y = 0$. Expressing s_0 in terms of p_0 and using Eq. (3) and the observation that $S_0 \propto s_0$ (Berzi and Fraccarollo, 2015), we obtain:

$$h = \frac{\Theta}{k_0 \bar{\nu} \cos\phi}\left(1 + \frac{1}{5}\frac{1}{2\sigma}\frac{1+2\nu_c}{1-\nu_c}\right)^{-1}. \tag{6}$$

The last term between parentheses in Eq. (6) represents the proportionality factor between the fluid and the particle shear stress at the bed. It differs from the expression reported in Berzi and Fraccarollo (2015) by the factor $1/5$, which permits to reproduce the dependence of the mass hold-up, $\bar{\nu}h$, on the Shields number and the angle of inclination measured in the 48 experiments of Capart and Fraccarollo (2011) (Fig. 3).

2.3. Determination of the distribution of pressure, p, in the solid phase

The balance of particle momentum along the y-direction, perpendicular to the flow, is (Berzi and Fraccarollo, 2013)

$$p' = -\nu\cos\phi, \tag{7}$$

where p is the particle pressure. Here, and in what follows, a prime indicates a derivative with respect to y. As mentioned, we have neglected the turbulent lift force associated with the correlation between the fluctuations of particle concentration and liquid velocity (McTigue, 1981). Integrating Eq. (7), with Eq. (1), gives

$$p = p_0 - h\left[\left(\frac{y}{h} + \frac{\exp E}{1-\exp E}\right)\nu - \frac{\nu_c}{E}\left(\frac{y}{h} + \frac{E\exp E}{1-\exp E}\right)\right]\cos\phi. \tag{8}$$

Eqs. (3) and (8) imply that the particle pressure vanishes at $y = h$.

2.4. Determination of the profile of the granular temperature, T

When collisions are the dominant source of stresses, the constitutive expression of the particle pressure can be expressed by the kinetic theory of hard, inelastic spheres. However, as suggested by Berzi et al. (2020), flows over erodible beds imply that the concentration must reach its critical value ν_c at the surface of the bed. This is possible only if the actual finite stiffness of the particles and the associated finite contact duration during collisions is accounted for, leading to Berzi and Jenkins (2015):

$$p = \nu\left[1 + 2\left(1+e_n\right)\nu\chi_0\right]T\left(1 + \frac{12}{5}\nu\chi_0\frac{T^{1/2}}{k_n^{1/2}}\right)^{-1}, \tag{9}$$

where χ_0, the radial distribution function at contact, is a function of ν which is singular at ν_c. For χ_0, we adopt the expression suggested by Vescovi et al. (2014):

$$\chi_0 = \left[1 - \theta(\nu-0.4)\left(\frac{\nu-0.4}{\nu_c-0.4}\right)^2\right]\frac{2-\nu}{2(1-\nu)^3} + \theta(\nu-0.4)\left(\frac{\nu-0.4}{\nu_c-0.4}\right)^2\frac{2}{\nu_c-\nu}, \tag{10}$$

in which $\theta(\cdot)$ is the Heaviside function.

In Eq. (9), T is the granular temperature, one-third of the mean square of the particle velocity fluctuations. The term between parentheses in Eq. (9) is the correction due to the finite contact duration, in which k_n is the dimensionless particle stiffness (Berzi and Jenkins, 2015).

With p and ν known at every y, Eq. (9) is a quadratic in the square root of the granular temperature that gives

$$T^{1/2} = \frac{6}{5k_n^{1/2}}\frac{p\chi_0}{1+2\left(1+e_n\right)\nu\chi_0} + \sqrt{\left[\frac{6}{5k_n^{1/2}}\frac{p\chi_0}{1+2\left(1+e_n\right)\nu\chi_0}\right]^2 + \frac{p}{\nu+2\left(1+e_n\right)\nu^2\chi_0}}. \tag{11}$$

2.5. Simultaneous determination of the granular shear stress distribution, s, and velocity profile, u, through the fluctuation kinetic energy balance for the solid phase

Once the distribution of the granular temperature is determined, we can employ the balance of fluctuation kinetic energy. For steady and fully-developed collisional granular-fluid flows, it reduces to Hsu et al. (2004)

$$-Q' + su' - \Gamma + \left(\frac{\sqrt{3}}{2}\sqrt{3T2K} - 3T\right)\frac{\nu}{\tau} = 0, \tag{12}$$

where: Q' is the diffusion of fluctuation kinetic energy associated with the particle agitation; su' is the production of fluctuation kinetic energy through the work of the particle shear stress; Γ is the rate of energy dissipation due to the inelastic nature of collisions; and the last term accounts for the particle agitation induced by the fluid turbulence (where K is the turbulent kinetic energy) and its suppression due to the drag (where τ is the particle relaxation time in the drag force, see Section 2.9) exerted by the fluid on the particles.

The rate of energy dissipation Γ term, in Eq. (12), reads (Berzi and Jenkins, 2015):

$$\Gamma = \frac{12\nu^2\chi_0\left(1-\epsilon^2\right)}{\pi^{1/2}L}T^{3/2}\left(1 + \frac{12}{5}\nu\chi_0\frac{T^{1/2}}{k_n^{1/2}}\right)^{-1}. \tag{13}$$

Here, L is the correlation length (Jenkins, 2006), which accounts for the fact that, at concentrations larger than the freezing point, 0.49 (Torquato, 1995), correlations in the fluctuation velocities of the particles develop (Mitarai and Nakanishi, 2007), thus reducing the energy dissipated in collisions. For simplicity, we employ the expression for the correlation length which has been determined from numerical simulations of homogeneous shearing flows (Berzi, 2014; Berzi and Vescovi, 2015):

$$L = 1 + \frac{26(1-\epsilon)}{15}\frac{\max(\nu-0.49,0)}{\nu_{rcp}-\nu}. \tag{14}$$

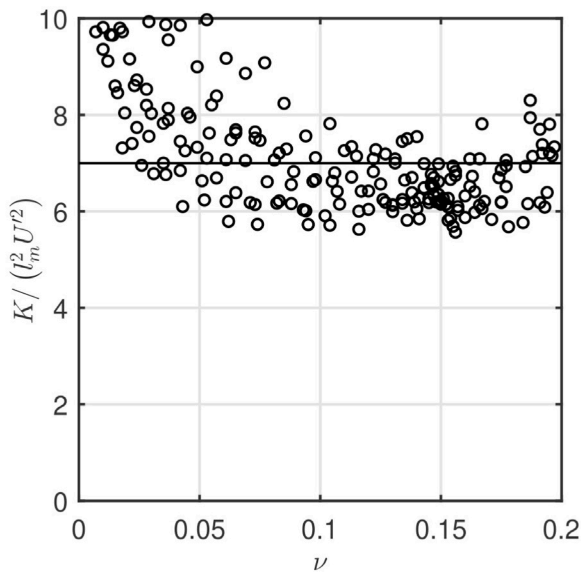

Fig. 4. Measured (circles, after Ni and Capart (2018)) scaled turbulent kinetic energy as a function of the solid volume fraction. The solid line is the assumed constant value equal to 7.

The term associated with the production of fluctuation energy due to fluid turbulence in Eq. (12) is taken to be proportional to $\sqrt{3T2K}$ rather than to $2K$ as in Hsu et al. (2004). We deem this more appropriate, given that it originates from the mean product of the fluid and particle velocity fluctuations, which are proportional to $\sqrt{3T}$ and $\sqrt{2K}$, respectively. In contrast, using $2K$ would imply that the particle velocity fluctuations scale with the turbulence intensity, which only applies when the particle inertia is small. In the spirit of a simple treatment of turbulence, we take the turbulent kinetic energy $K \propto l_m^2 U'^2$, with l_m, the mixing length and U the fluid velocity in the x-direction. The mixing length is one of the specific closures presented in the Section 2.9. Ni and Capart (2018) have performed measurements of the average of the product of the fluid velocity fluctuations on mild sediment transport of 7 mm plastic particles, thus permitting to plot the ratio $K/\left(l_m^2 U'^2\right)$ as a function of the solid volume fraction (Fig. 4). Taking $K \approx 7 l_m^2 U'^2$ permits to capture the data reasonably well. With this, the numerical factor $\sqrt{3}/2$ in front of $\sqrt{3T2K}$ in Eq. (12) permits to reproduce the experimental finding (Berzi and Fraccarollo, 2015) that $T = 3.5 l_m^2 U'^2$ in the dilute part of the flow, where we expect that there is a balance between the production of particle velocity fluctuations induced by the fluid and their dissipation through the drag. We assume, for simplicity, as in Berzi and Fraccarollo (2015), that the energy diffusion in Eq. (12) is negligible. We can easily remove this assumption and make use of the constitutive relation of the flux of fluctuation kinetic energy of the kinetic theory (Garzó and Dufty, 1999), if deemed necessary.

Following Garzó et al. (2012), we include the influence of the fluid drag in the constitutive relation for the particle shear stress, and express it, as in Chassagne et al. (2023), as:

$$s = \left[\left(\frac{1}{\eta_k} + \frac{1}{\eta_D}\right)^{-1} + \eta_c\right] u', \tag{15}$$

where:

$$\eta_k = \frac{8 J_k \nu^2 \chi_0 T^{1/2}}{5\pi^{1/2}} \left(1 + \frac{12}{5}\nu\chi_0 \frac{T^{1/2}}{k_n^{1/2}}\right)^{-1} \tag{16}$$

is the granular viscosity associated with the streaming contribution to the momentum exchange, modified to include the finite duration of contacts (Berzi and Jenkins, 2015);

$$\eta_D = \tau \nu T \tag{17}$$

is the granular viscosity due to the fluid drag in between collisions (Jenkins et al., 2010; Garzó et al., 2012), and

$$\eta_c = \frac{8 J_c \nu^2 \chi_0 T^{1/2}}{5\pi^{1/2}} \left(1 + \frac{12}{5}\nu\chi_0 \frac{T^{1/2}}{k_n^{1/2}}\right)^{-1} \tag{18}$$

is the granular viscosity associated with the collisional contribution to the momentum exchange, modified to include the finite duration of contacts (Berzi and Jenkins, 2015). The coefficients J_k and J_c can be obtained from Garzó and Dufty (1999) as

$$J_k = \frac{5\pi}{32\nu^2\chi_0^2} \frac{5 + 2\left(1+e_n\right)\left(3e_n - 1\right)\nu\chi_0}{24 - 6\left(1-e_n\right)^2 - 5\left(1-e_n^2\right)} \left[1 + \frac{\pi}{12}\frac{3e_n - 1}{3 - e_n}\right], \tag{19}$$

and

$$J_c = \left\{\frac{1+e_n}{2} + \frac{\pi\left(1+e_n\right)}{8\nu\chi_0} \frac{5 + 2\left(1+e_n\right)\left(3e_n - 1\right)\nu\chi_0}{24 - 6\left(1-e_n\right)^2 - 5\left(1-e_n^2\right)}\right\} \times \left[1 + \frac{\pi}{12}\frac{3e_n - 1}{3 - e_n}\right], \tag{20}$$

respectively, where the factor between square brackets has been determined in Saha and Alam (2016) as the lowest order correction to the shear stress that captures the anisotropy in the single-particle velocity distribution function (Jenkins and Richman, 1988).

Using Eq. (15) into Eq. (12), neglecting Q' and assuming for simplicity that $u' \simeq U'$, so that $K \simeq 7{l_m}^2 u'^2$, permit to re-write Eq. (12) as a quadratic equation in the particle strain rate, u',

$$\left[\left(\frac{1}{\eta_k} + \frac{1}{\eta_D}\right)^{-1} + \eta_c\right] u'^2 + \frac{\sqrt{21}}{2}\sqrt{6T}\, l_m \frac{\nu}{\tau} u' - \Gamma - 3\frac{\nu}{\tau} T = 0, \tag{21}$$

which can then be calculated at every position inside the transport layer, once closures for the mixing length l_m and the relaxation time τ are provided (see Section 2.9). Then, with Eq. (15), we can obtain the distribution of the particle shear stress.

With u' known at every position y, we can numerically solve by quadrature the integral $u = \int_0^y u' \mathrm{d}y$, with the boundary conditions $u = 0$ at the surface of the bed ($y = 0$), to obtain the velocity distribution of the particles in the transport layer. The particle velocity at the surface of the bed is actually nonzero because the bed creeps (Komatsu et al., 2001). However, the contribution of the creep motion of the particles inside the bed to the total transport rate can be ignored (Berzi et al., 2020).

2.6. Determination of the total flow depth, H, and the distribution of the fluid shear stress, S

The momentum balance of the mixture in the flow direction (Berzi and Fraccarollo, 2013) permits the determination of the distribution of the fluid shear stress in the transport layer and in the clear fluid region above it,

$$S = \frac{H - y}{\sigma - 1}\sin\phi + p\tan\phi - s, \tag{22}$$

with $p = s = 0$ for $y \geq h$. Then, the total flow depth H can be obtained by taking $s + S = \Theta$ at the surface of the bed in Eq. (22), so that, with Eq. (3),

$$H = \frac{\sigma - 1}{\sin\phi}\Theta - (\sigma - 1)\bar{\nu} h. \tag{23}$$

As suggested by Berzi and Fraccarollo (2015), we take the fluid shear stress to be the sum of two contributions: one associated with turbulence, which we describe using the aforementioned mixing length approach; and one associated with momentum exchange induced by particle agitation, with the corresponding viscosity proportional to the granular viscosity. Then,

$$S = \frac{1-\nu}{\sigma} l_m^2 U'^2 + \frac{1}{5}\frac{1+2\nu}{2\sigma(1-\nu)}\left[\left(\frac{1}{\eta_k}+\frac{1}{\eta_D}\right)^{-1} + \eta_c\right] U'. \tag{24}$$

The pre-factor in front of the granular viscosity, s/u' (see Eq. (15)), in the second term of the right-hand side of Eq. (24), is the concentration-dependent coefficient of proportionality that we have already employed in the determination of the depth of the transport layer (Eq. (6)).

With the distribution of the fluid shear stress given by Eq. (22), the fluid shear rate, U', can be determined by solving the quadratic Eq. (24). Then, with U' known at any position, we can numerically solve by quadrature the integral $U = \int_0^y U' \mathrm{d}y$, with the boundary conditions, $U = U_0$ (see later) at the surface of the bed, to obtain the fluid velocity distribution in the transport layer.

2.7. Determination of the distribution of the drag force, D, from the conservation of the momentum for the fluid in the flow direction

The momentum balance for the fluid in the flow direction (Berzi and Fraccarollo, 2013) permits the determination of the distribution of the drag, D, exerted by the fluid on the particles as

$$D = \frac{1-\nu}{\sigma-1}\sin\phi + S', \tag{25}$$

where the derivative of the fluid shear stress must be calculated numerically from the distribution of S in the transport layer.

We model the drag as (Jenkins and Hanes, 1998)

$$D = \frac{\nu}{\tau}(U-u). \tag{26}$$

Using Eq. (25) in Eq. (26), and ignoring the derivative of the fluid shear stress at the surface of the erodible bed, permits us to determine U_0 there as

$$U_0 = \frac{\tau_0}{\sigma-1}\frac{1-\nu_c}{18\nu_c}\sin\phi, \tag{27}$$

where τ_0 is the particle relaxation time (see Section 2.9) evaluated at the bed. Eq. (27) is the equivalent of Darcy's law (Whitaker, 1986) to evaluate the fluid velocity in a porous medium, when gravity is the sole driving force.

2.8. The theoretical determination of the optimum concentration parameter, E^*

The full solution of the hydrodynamic variables requires as input, for a given particle-liquid system, the angle of inclination of the bed, ϕ, the Shields number, Θ, and the concentration parameter, E. These three degrees of freedom are at odds with the experimental evidence (Capart and Fraccarollo, 2011) that there are only two degrees of freedom: steady, fully developed, inclined flows of particles and liquid over erodible beds are completely determined once the angle of inclination of the bed and the Shields number - or, equivalently, the particle and liquid flow rates - are assigned. E can be selected in a wide range of values (Fig. 2). To eliminate the additional degree of freedom, we choose the concentration parameter, for a given combination of ϕ and Θ, as the optimum value E^* for which $H > h$ and which minimizes the mean variance of the residuals between the drag force distribution determined by the momentum balance (Eq. (25)) and that determined by its constitutive relation (Eq. (26)). This mean variance is calculated in the region, whose thickness is at least one diameter, where the mean free path is less than the length of the ballistic trajectory (see the later Eq. (30)).

We emphasize that this process does not imply any fitting against experimental data. We do not obtain the concentration profile from the conservation laws, but assume an arbitrary analytical form of it which depends on E. Hence, the drag force obtained from the momentum balance (Eq. (25)) and that obtained from its constitutive relation (Eq. (26)) may coincide at most locally in the sediment layer, not everywhere throughout it. Therefore, the optimum value $E^*(\phi, \Theta)$ is the one that minimizes this inconsistency throughout the sediment layer. When $E = E^*$, the mean residual between Eqs. (25) and (26) is about 50% of the mean drag obtained from the momentum balance (at least for the experimental conditions considered in the present work).

2.9. Closures for the particle relaxation time and the mixing length

2.9.1. Particle relaxation time, τ

For simplicity, we take the particle relaxation time to be

$$\tau = \left[\frac{3}{4}\frac{24}{\sigma \mathrm{R}}\frac{1}{(1-\nu)^{n-2}}\right]^{-1}, \tag{28}$$

that is the relaxation time in the case of Stokes drag, with the concentration dependence suggested by Richardson and Zaki (1954) in the case of small relative velocity between the particles and the fluid (Felice, 1995; Chauchat, 2018); the exponent n depends on the product $\sigma\mathrm{R}^2$, and equals 2.4 as $\sigma\mathrm{R}^2 \rightarrow \infty$ (Felice, 1995). We emphasize that the coefficient 24 in Eq. (28) is appropriate for spheres. More complicated expressions for the particle relaxation time are possible but would make our model implicit (and the description of its solution less straightforward). In any case, we have checked that changing the particle relaxation time has minimal effects on the profiles of particle velocity and granular temperature. On the other hand, the fluid velocity profile is more sensitive to it, but experimental data are lacking, making at this stage pointless the implementation of more refined expressions for τ.

2.9.2. Mixing length, l_m

Berzi and Fraccarollo (2015) have found that the mixing length in collisional suspensions, at concentrations larger than 0.2, is only a function of the concentration itself, implying that the size of the inter-particle gap constrains the size of the turbulent eddies. However, when the concentration is less than 0.2, the size of the turbulent structures should increase and, eventually, we should recover the classical result that the mixing length increases linearly with the distance from some reference position, being the von Kármán constant, $\kappa = 0.41$, the coefficient of proportionality. In fact, as shown by Revil-Baudard et al. (2015), the influence of the sediments on the mixing length extends well beyond the transport layer, in a region where the concentration is negligible. Revil-Baudard et al. (2015) proposed to change the von Kármán constant to the reduced value of 0.225 to account for this phenomenon. However, in doing so, they cannot recover the classical expression for the mixing length in the absence of sediments. Here, we propose the following expression for the mixing length

$$l_m = 3\left(\nu_{rcp}-\nu\right)^3 + \kappa y\left[1-\exp\left(-0.3\frac{y}{h}\right)\right], \tag{29}$$

where the first term on the right-hand side of Eq. (29) is the local mixing length suggested by Berzi and Fraccarollo (2015) in the case of 3.35 mm plastic particles in water. Local refers to the fact that the turbulence originates at the surface of the grains located at y and the size of the turbulent eddies is limited by the spacing between them. Ni and Capart (2018) found that this expression over-predicts the mixing length in the case of 7 mm plastic particles. Hence, the numerical factor in front of $\left(\nu_{rcp}-\nu\right)^3$ likely depends on the particle inertia over the intensity of the fluid turbulence: the more massive are the particles, the more effective they are in suppressing the fluid turbulence.

The second term on the right-hand side of Eq. (29) represents the nonlocal growth of the mixing length, in which we have introduced the damping factor, $1-\exp(-0.3y/h)$, in the spirit of Van Driest's model of turbulence (Van Driest, 1956), where the thickness of the transport layer is the natural length scale for the damping of the eddies in the presence of sediments. Nonlocal means that the origin of the turbulence

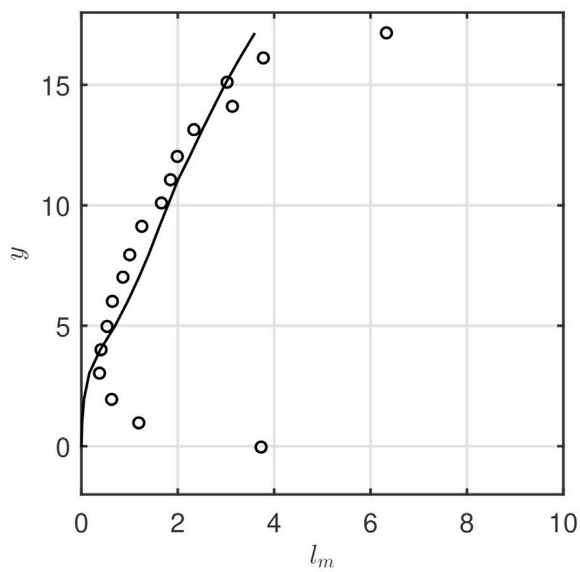

Fig. 5. Measured (circles, after Revil-Baudard et al. (2015)) and predicted (line, Eq. (29), with $\nu_{rcp} = 0.64$ and $h = 10$) mixing length as a function of the distance from the erodible bed.

is different from the local position y, and that the size of the eddies grows accordingly. Fig. 5 shows that Eq. (29) can reproduce the values of the mixing length measured in the experiments (Revil-Baudard et al., 2015). The increase of the mixing length near the erodible bed is a signature of the component of the fluid viscosity associated with the particle agitation (Eq. (24)).

2.10. Limitations of the present approach

2.10.1. The presence of a ballistic region in the sediment transport layer

As pointed out by Pasini and Jenkins (2005), the constitutive relations for the particle stresses of the kinetic theory are valid if the mean free path - the mean distance covered by a particle in between two successive collisions - is less than the typical length of a ballistic trajectory - the path followed by a particle under the influence of gravity and, in the present case, buoyancy and drag. With the expression of the mean free path of kinetic theory (Chapman and Cowling, 1970), and the length of a ballistic trajectory approximated as twice the maximum height reached by a saltating particle determined by Valance and Berzi (2022) in terms of the drag relaxation time and the granular temperature, this criterion translates into

$$2\tau\sqrt{2T} - 2\tau^2 \ln\left(\frac{\sqrt{2T}}{\tau} + 1\right) > \frac{\sqrt{2}}{12\nu\chi_0}. \tag{30}$$

We might conjecture that, even if the length of a ballistic trajectory is larger than the mean free path, there is a layer in which the two quantities have similar values, thus indicating the existence of a transitional regime between purely collisional and purely ballistic.

The criterion of Eq. (30) will be applied to the analytical results for the flow conditions of Capart and Fraccarollo (2011), to determine which portion of the transport layer is actually characterized by a mixture of ballistic and collisional behaviour. It is already known that, in the cases of aeolian transport (Pasini and Jenkins, 2005) and gravity-driven dry granular flows (Berzi et al., 2020), the contribution of the ballistic layer to the total transport is negligible.

We emphasize once again that our determination of the optimum concentration parameter is based on minimizing the inconsistency between the drag force evaluated from the momentum balance and its constitutive relation only in the portion of the sediment layer where Eq. (30) is satisfied. Then, our approach is not adequate when the criterion of Eq. (30) is not satisfied in a significant portion of the transport layer (say greater than 20%–30%).

2.10.2. Unphysical consequences of the logarithmic concentration profile in the dilute part of the transport layer

Another limitation is associated with the arbitrary choice of the analytical concentration profile (Eq. (1)). Irrespectively of the parameter E, the Shields number, and the angle of inclination, Eq. (11) implies that the granular temperature decreases near the top of the transport layer, where the concentration is small. Experiments and discrete simulations of flows of granular-fluid mixtures and dry granular materials over erodible beds show, instead, that the granular temperature monotonically increases with the distance from the bed (Armanini et al., 2005; Berzi and Fraccarollo, 2015; Berzi et al., 2020), eventually saturating and becoming independent of y in the ballistic layer (Pasini and Jenkins, 2005). In the dilute limit, $p = \nu T$ (Garzó and Dufty, 1999), and, with Eq. (7), we obtain

$$T' = \left(-\frac{\nu' \int \nu \mathrm{d}y}{h\nu^2} - 1\right)\cos\phi. \tag{31}$$

In order to agree with the experimental observation that $T' \geq 0$ near the top, then it is necessary that

$$-\nu' \frac{1}{h}\int \nu \mathrm{d}y \geq \nu^2. \tag{32}$$

It can be easily shown that this condition cannot be satisfied by the logarithmic distribution of the concentration of Eq. (1), implying that the probabilistic assumptions of Lien and Tsai (2003) are not satisfied, at least near the top of the transport layer. There, only an exponential distribution of the concentration, such as that typical of saltation (Creyssels et al., 2009), the dominant mode of transport for wind-blown sand, is compatible with a uniform distribution of the granular temperature ($T' = 0$). However, despite the nonphysical consequence of Eq. (1) for the distribution of the granular temperature near the top of the transport layer, we will show that the rest of the hydrodynamic variables can be reasonably well predicted assuming its validity throughout the flow.

2.11. Differences and similarities with Chassagne et al. (2023)

There are clearly similarities between the present model and the model of Chassagne et al. (2023), which is an indication of the central role of the kinetic theory of granular gases in two-phase approaches to intense sediment transport. Indeed, both models employ the constitutive relations for the particle stresses and the collisional rate of dissipation of the fluctuation kinetic energy derived by Garzó and Dufty (1999), with an effective coefficient of restitution which permits the inclusion of the role of friction in the energy dissipation.

Both models include the influence of the fluid drag on the constitutive relation for the particle viscosity, although Chassagne et al. (2023) claim that this is sufficient to account for the presence of a ballistic layer on top of the collisional layer. As shown in Berzi et al. (2024), the influence of drag, buoyancy and gravity in between collisions cannot be fully captured using Eq. (17). More work is required to understand the transition from collisionless to collisional saltation and, then, to collisional suspension, and this seems to be particularly important in the case of aquatic sediment transport.

Chassagne et al. (2023) assume that the particle total stress is the sum of an inertial and an elastic component, and also assume that the elastic shear stress is proportional through a Coulomb coefficient to the elastic pressure. They activate the elastic components when the concentration reaches a value (improperly named random loose packing) which is less than the value at which the functions of the kinetic theory for rigid particles diverge (the critical concentration ν_c of the present work). First, the random loose packing is simply the critical concentration for particle friction equal to infinity (Silbert,

2010) and has no particular meaning for finite friction. Second, as detailed in Berzi (2024), elastic components of the stresses arise only when the concentration is larger than the critical, and, therefore, they are not needed to model the flow above an erodible bed.

In the present model, we include the roles of velocity correlation and finite contact duration on the constitutive relations of kinetic theory, ignored in Chassagne et al. (2023). These permit to predict the value of the stress ratio at the bed solely on the basis of the microscopic contact parameters of the particles, and to regularize the singularities in the constitutive relations of kinetic theory at the critical concentration.

Different expressions for the radial distribution function at contact are adopted here and in Chassagne et al. (2023). However, they are both consistent with Carnahan and Starling (1969) at low concentrations, and diverge as $\nu \rightarrow \nu_c$. In the absence of direct and extensive measurements in discrete simulations, they are both equally valid.

The expressions for the turbulent mixing length and the particle relaxation time are different in the two models. We also include an additional, granular-like term in the fluid viscosity associated with the momentum exchange induced by particle agitation (Berzi and Fraccarollo, 2015), not present in Chassagne et al. (2023). The latter is necessary to explain the increase of fluid viscosity near the bed (Fig. 4), where the large concentration should suppress the fluid turbulence. However, only fully-resolved numerical simulations (Vowinckel et al., 2014) of the fluid surrounding the particles in intense sediment transport would provide final answers on how to model the fluid viscosity as well as the drag.

The present model accounts for the source of particle fluctuations induced by the fluid turbulence, ignored in Chassagne et al. (2023), while neglecting the fluctuation energy diffusion associated with particle agitation, accounted for in Chassagne et al. (2023). A more complete model should include both.

Finally, and crucially, we assume in our model an analytical concentration profile, while Chassagne et al. (2023) solve for it. Hence, in the present work, only an approximate solution can be determined, in which the drag force from its constitutive relation and that from the momentum balance differ by a certain amount. However, the solution is almost entirely analytical, at virtually no computational cost. The solution of the model proposed by Chassagne et al. (2023), which is 'exact' in the sense that the profiles of all the variables of the problem are determined on the basis of balance equations, constitutive relations and boundary conditions, is instead computationally demanding.

3. Results and comparisons

Here, we make comparisons between the results of the present theory and the experiments performed by Capart and Fraccarollo (2011) with water and plastic cylinders having length-to-diameter ratio equal to 0.8 and diameter of the equivalent sphere equal to 3.35 mm, $\sigma = 1.51$ and $\mathrm{R} = 370$. With $\sigma \mathrm{R}^2 \approx 2 \cdot 10^5$, the exponent n in Eq. (28) is equal to 2.4 (Richardson and Zaki, 1954). The experiments were performed in a rectangular channel, covering a range of Shields numbers from 0.4 to 2.8, and angles of inclination of the erodible bed from $0.6°$ to $4.5°$. We take the coefficients of restitution and friction from the measurements of the impact of two Delrin spheres reported in Foerster et al. (1994): $e_n = 0.97, e_t = 0.44$ and $\mu = 0.2$. With these, the calculations suggested by Larcher and Jenkins (2013) give an effective coefficient of restitution $\varepsilon = 0.77$. The discrete numerical simulations of steady, simple shearing of true cylinders reported by Berzi et al. (2022) indicate that the critical volume fraction ν_c is 0.61, and that the random close packing ν_{rcp} is 0.68 for cylinders with aspect ratio equal to 0.8 and friction equal to 0.2. Finally, Young's modulus of plastic translates into a dimensionless stiffness k_n approximately equal to 10^8. In experimental measurements, as explained in Capart and Fraccarollo (2011), the position of the top of the erodible bed and the origin of the y axis were established where the velocity of the particles in the x direction falls below the sensitivity limit of the tools used to determine it. This conflicts with the criterion $\nu = \nu_c$ that we employ to identify the erodible bed in the previously described semi-analytical treatment based on the kinetic theory, and must be kept in mind when assessing the agreement between the theory and the experiments.

We have first determined the optimum concentration parameter, E^*, for different combinations of the Shields number and the angle of inclination of the erodible bed in the case of plastic cylinders transported in water. We expect that E^* is roughly independent of the Shields number. This would be consistent with the experimental findings that the ratio H/h is only a function of the angle of inclination (Berzi and Fraccarollo, 2013). In fact, the ratio of Eqs. (6) and (23) suggests that, given the particle and fluid properties, $\bar{\nu}$ is a function of ϕ and H/h. Given that $\bar{\nu}$ only depends on E (Eq. (2)), H/h is solely a function of ϕ if also the optimum entropic parameter depends on ϕ only.

The dependence of E^* on the angle of inclination is depicted in Fig. 6a. In the inset of the plot, we also show the percentage of the sediment layer in which the criterion of Eq. (30) is satisfied as a function of the angle of inclination of the bed. It turns out that many of the experiments carried out by Capart and Fraccarollo (2011) are significantly affected by the ballistic motion of the particles. When more than 70% of the sediment layer is characterized by purely collisional behaviour, that is, when ϕ is greater than $3°$, E^* increases linearly with ϕ, indicating that more convex concentration profiles are associated with steeper flows. In Fig. 6b, we compare the mean concentration measured in the experiments and that predicted using Eq. (2), with $E = E^*$. The mean concentration is reasonably well predicted by the optimum entropic parameter.

Fig. 7 depicts the theoretical profiles of the particle, liquid and total shear stresses in the transport layer for assigned input values of ϕ and Θ. Here and in what follows, unless otherwise stated, the results of the theory refer only to the region of the flow for which the criterion given by Eq. (30) is satisfied. The particle shear stress decreases towards the top of the transport layer, where it vanishes, and reaches a maximum slightly above the interface with the erodible bed. This maximum corresponds to a local minimum in the liquid shear stress. The latter is due to the competition between the two components of the fluid shear stress (Eq. (24)): the liquid turbulence decreases when the particle concentration increases, while the momentum exchange induced by the particle agitation increases towards the bed. At the bottom ($y = 0$), the total shear stress is equal to the Shields parameter.

Fig. 8 illustrates the comparisons between the experiments and the theoretical predictions in terms of profiles of concentration, particle velocity, and granular temperature for four of the runs performed by Capart and Fraccarollo (2011). Similar results, not shown here for brevity, are obtained for the rest of the experimental runs with intense sediment transport. Although the model predictions of the granular temperature and particle and fluid velocities are limited to the collisional layer, the concentration profile is reported for the entire transport layer, including the ballistic layer at the top.

The agreement between the measured and predicted granular temperature is notable. The concentration is well predicted where collisions dominate and poorly predicted in the ballistic layer on top of the collisional layer, where we anticipated the failure of the entropic approach. The upper part of the velocity profile of the particles is slightly underestimated. This is likely due to the transition from collisional to ballistic layer, which is currently not considered in the constitutive relation of particle shear stress (Eq. (15)).

A striking feature of sediment transport in water is that the concentration at the top of the collisional layer, where the mean free path equals the length of the ballistic trajectory (recognizable in Fig. 8 as the upper limit of the predicted profiles of granular temperature, and particle and fluid velocity), is about 0.1 to 0.2. That means that in a significant portion of the transport layer, the trajectories of the particles between collisions are strongly affected by external forces

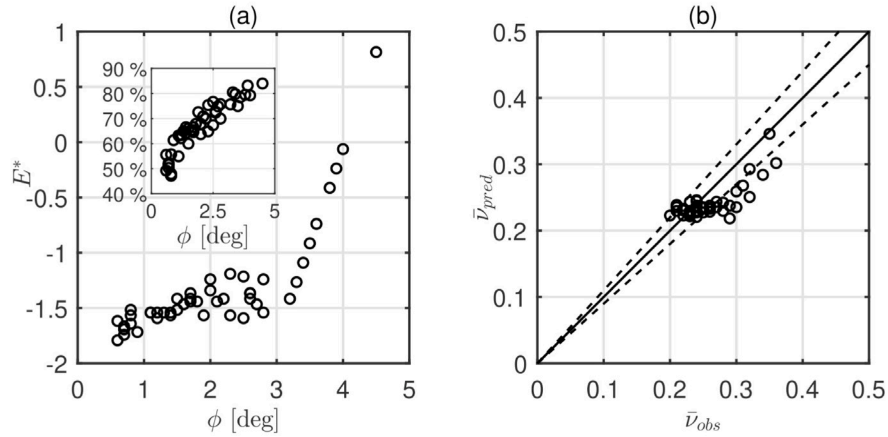

Fig. 6. (a) Optimum entropic parameter (circles) as a function of the angle of inclination of the bed in the case of sediment transport of plastic cylinders in water. The inset depicts the percentage of the sediment layer with purely collisional behaviour (where Eq. (30) is satisfied) as a function of the angle of inclination of the bed. (b) Predicted (Eq. (2) with the optimum E from (a)) versus observed mean solid volume fraction in the case of sediment transport of plastic cylinders in water. Also shown are the perfect fit (solid line) and the $\pm 10\%$ confidence interval (dashed lines).

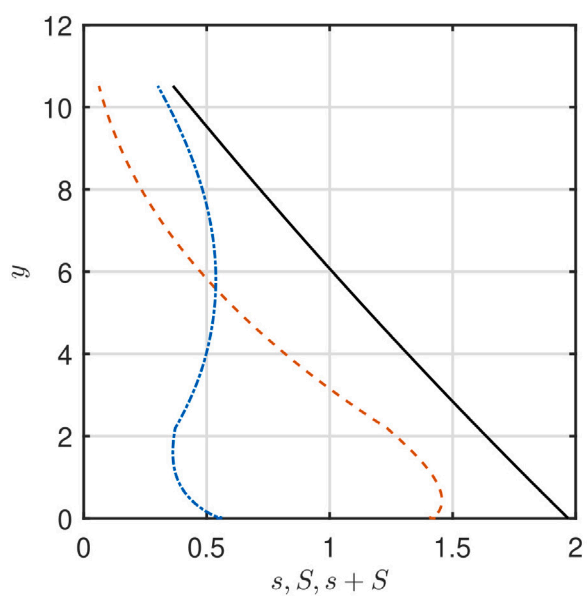

Fig. 7. Profiles of particle (orange dashed line), liquid (blue dot-dashed line) and total (black solid line) shear stress in the transport layer for $\phi = 3.8°$ and $\Theta = 2$, with $E^* = -0.41$.

such as gravity, buoyancy, and drag. Once again, this is very different from both dry inclined granular flows (Berzi et al., 2020) and aeolian transport (Pasini and Jenkins, 2005), where collisions are dominant and, therefore, the kinetic theory of granular gases is relevant even at values of the particle concentration as low as 0.01, one order of magnitude less than the present case of aquatic transport.

Although not measured in the experiments, we also show in Fig. 8 the theoretical profiles of the liquid velocity in the flow direction. The resulting velocity difference is such that the Reynolds number based on it, that is, $(U-u)\,\mathrm{R}$, is larger than unity. Then, the particle relaxation time based on Stokes drag is not appropriate and one should have used a more complicated expression that includes both Stokes and form drag (Felice, 1995; Chauchat, 2018). However, as mentioned, only the fluid velocity profile is sensitive to it, while the optimum concentration parameter, the particle velocity and the granular temperature are unaffected, at least when the portion of the sediment layer dominated by collisions is larger than 70%.

4. Concluding remarks

In this paper, the steady, inclined, collisional flow of sediments immersed in a turbulent liquid over an erodible bed has been modelled in the frame of the kinetic theory of granular gases. In doing so, we have accounted for particle surface friction, cylindrical shape, finite-duration of contacts, exchange between turbulent kinetic energy and fluctuation kinetic energy of the particles, suppression of turbulence due to the presence of the particles and fluid momentum exchange induced by particle agitation.

The complicated set of differential equations composed of balances of momentum and energy, closed by a series of constitutive relations, has been solved semi-analytically by assuming that the particle concentration followed an arbitrary, single-parameter logarithmic distribution. The parameter of the distribution has been determined by minimizing the difference between the analytical profiles of the drag force obtained from the fluid momentum balance and its constitutive relation, without any experimental fitting. We have shown that the optimum entropic parameter grows linearly with the angle of inclination of the bed, at least when the portion of the sediment layer dominated by collisions is larger than 70%.

We have determined the profiles of particle and liquid shear stresses, velocities, and granular temperature and made successful comparisons against experimental measurements on the transport of plastic cylinders in water for a range of bed slopes and intensity of the shearing. We have seen that, unlike the case of aeolian transport, in a significant upper part of the transport layer, the length of the particle trajectories influenced by external forces (gravity, buoyancy, and drag) in between successive collisions is shorter or of the same order of magnitude than the mean free path of kinetic theory. Hence, the ballistic motion plays a significant role even in the case of intense sediment transport when the carrier fluid is water.

Other analytical forms of the concentration profile could have been employed, perhaps leading to improvements in the present approach. Further improvements could have been obtained by relaxing some of the assumptions, such as the equality of the particle and liquid shear rate throughout the flow, and the usage of a particle relaxation time appropriated for Stokes drag.

Finally, our analysis has permitted to highlight which are the open issues that need to be addressed before any claims on the existence of a state-of-the-art, comprehensive mathematical model of unidirectional, intense sediment transport: (i) the lack of a physically sound model for the ballistic-collisional motion of particles in the upper portion of

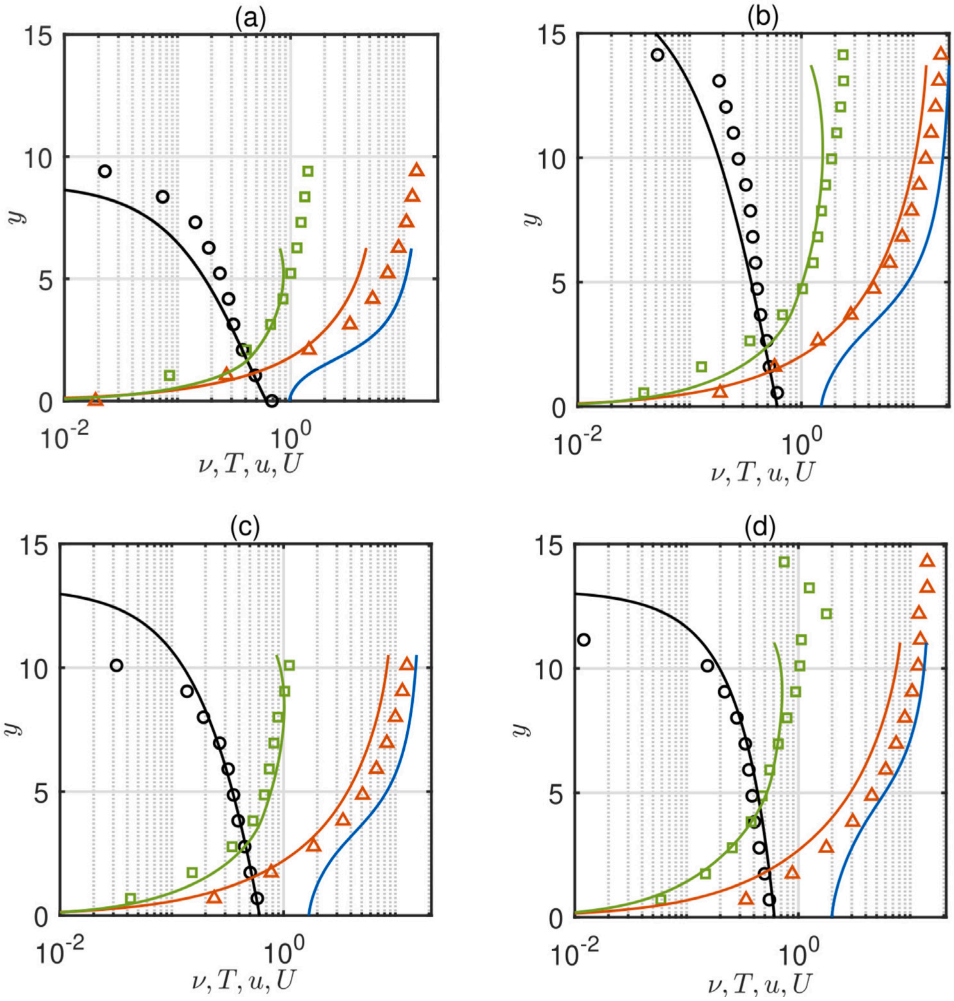

Fig. 8. Experimental measurements (symbols) and theoretical predictions (lines) of profiles of concentration (black lines and circles), particle (orange lines and triangles) and liquid (blue lines) velocity, and granular temperature (green lines and squares) when: (a) $\phi = 2.2°$ and $\Theta = 1.1$, with the corresponding optimum $E^* = -1.42$; (b) $\phi = 3.4°$ and $\Theta = 2.3$, with the corresponding optimum $E^* = -1.09$; (c) $\phi = 3.8°$ and $\Theta = 2.0$, with the corresponding optimum $E^* = -0.41$; (d) $\phi = 4.5°$ and $\Theta = 2.4$, with the corresponding optimum $E^* = 0.81$. (For interpretation of the references to colour in this figure legend, the reader is referred to the web version of this article.)

the sediment layer that is crucial in aquatic condition; (ii) the lack of experimental data for phrasing accurate expressions for the mixing length as a function of the sediments and fluid properties; (iii) the lack of experimental measurements for expressing the turbulent kinetic energy in terms of the mixing length; (iv) the need for discrete element simulations of the particles coupled to direct numerical simulations for the surrounding fluid, e.g., to confirm the existence and the model of the granular-like component of the fluid viscosity.

CRediT authorship contribution statement

Diego Berzi: Writing – review & editing, Writing – original draft, Methodology, Formal analysis, Conceptualization. **Ashkan Pilbala:** Writing – review & editing, Visualization, Investigation. **Luigi Fraccarollo:** Writing – review & editing, Writing – original draft, Methodology, Formal analysis, Conceptualization.

Financial support

This research has been supported by the Ministero dell'Istruzione, dell'Università e della Ricerca (grant no. 2017SEB7Z8), Project ''Enterprising''.

Declaration of competing interest

The authors declare the following financial interests/personal relationships which may be considered as potential competing interests: Luigi fraccarollo reports financial support was provided by MUR, Italian Ministry of Research. The other authors declare that they have no known competing financial interests or personal relationships that could have appeared to influence the work reported in this paper.

Data availability

Data will be made available on request.

References

Andreotti, Bruno, 2004. A two-species model of aeolian sand transport. J. Fluid Mech. (ISSN: 0022-1120) 510, 47–70. http://dx.doi.org/10.1017/S0022112004009073,

Armanini, Aronne, Capart, Hervé, Fraccarollo, Luigi, Larcher, Michele, 2005. Rheological stratification in experimental free-surface flows of granular–liquid mixtures. J. Fluid Mech. (ISSN: 0022-1120) 532, 269–319. http://dx.doi.org/10.1017/S0022112005004283, URL http://www.journals.cambridge.org/abstract_S0022112005004283.

Bagnold, R.A., 1941. The Physics of Blown Sand and Desert Dunes. Methuen, New York.

Berzi, Diego, 2011. Analytical solution of collisional sheet flows. J. Hydraul. Eng. - ASCE 137 (10), 1200–1207. http://dx.doi.org/10.1061/(ASCE)HY.1943-7900.0000420, URL http://cat.inist.fr/?aModele=afficheN&cpsidt=24746740.

Berzi, Diego, 2014. Extended kinetic theory applied to dense, granular, simple shear flows. Acta Mech. (ISSN: 0001-5970) 225 (8), 2191–2198. http://dx.doi.org/10.1007/s00707-014-1125-1, URL http://link.springer.com/10.1007/s00707-014-1125-1.

Berzi, Diego, 2024. On granular flows : From kinetic theory to inertial rheology and nonlocal constitutive models. Phys. Rev. Fluids 9, 034304. http://dx.doi.org/10.1103/PhysRevFluids.9.034304.

Berzi, Diego, Buettner, Kevin E., Curtis, Jennifer S., 2022. Dense shearing flows of soft, frictional cylinders. Soft Matter (ISSN: 17446848) 18 (1), 80–88. http://dx.doi.org/10.1039/d1sm01395e, URL http://dx.doi.org/10.1039/d1sm01395e.

Berzi, Diego, Fraccarollo, Luigi, 2013. Inclined, collisional sediment transport. Phys. Fluids 25 (10), 106601. http://dx.doi.org/10.1063/1.4823857.

Berzi, Diego, Fraccarollo, Luigi, 2015. Turbulence locality and granularlike fluid shear viscosity in collisional suspensions. Phys. Rev. Lett. (ISSN: 0031-9007) 115, 194501. http://dx.doi.org/10.1103/PhysRevLett.115.194501.

Berzi, Diego, Fraccarollo, Luigi, 2016. Intense sediment transport: Collisional to turbulent suspension. Phys. Fluids (ISSN: 1070-6631) 28 (2), 023302. http://dx.doi.org/10.1063/1.4941770, URL http://scitation.aip.org/content/aip/journal/pof2/28/2/10.1063/1.4941770.

Berzi, Diego, Jenkins, James T., 2015. Steady shearing flows of deformable, inelastic spheres. Soft Matter (ISSN: 10706631) 11 (24), 4799–4808. http://dx.doi.org/10.1039/C5SM00337G, URL http://dx.doi.org/10.1039/C5SM00337G.

Berzi, Diego, Jenkins, James T., Richard, Patrick, 2019. Erodible, granular beds are fragile. Soft Matter (ISSN: 1744-683X) 15, 7173–7178. http://dx.doi.org/10.1039/c9sm01372e, URL http://dx.doi.org/10.1039/C9SM01372E.

Berzi, Diego, Jenkins, James T., Richard, Patrick, 2020. Extended kinetic theory for granular flow over and within an inclined erodible bed. J. Fluid Mech. 885, A27. http://dx.doi.org/10.1017/jfm.2019.1017.

Berzi, Diego, Valance, Alexandre, Jenkins, James T., 2024. Collisionless kinetic theory for saltation over a rigid, bumpy bed. J. Fluid Mech. 991, A15.

Berzi, Diego, Vescovi, Dalila, 2015. Different singularities in the functions of extended kinetic theory at the origin of the yield stress in granular flows. Phys. Fluids (1994-Present) 27 (1), 013302. http://dx.doi.org/10.1063/1.4905461.

Capart, Hervé, Fraccarollo, Luigi, 2011. Transport layer structure in intense bed-load. Geophys. Res. Lett. (ISSN: 0094-8276) 38, L20402. http://dx.doi.org/10.1029/2011GL049408, URL http://www.agu.org/pubs/crossref/2011/2011GL049408.shtml.

Carnahan, N.F:, Starling, K.E., 1969. Equation of state for nonattracting rigid spheres. J. Chem. Phys. 51 (2), 635–636. http://dx.doi.org/10.1063/1.1672048.

Chapman, S., Cowling, T.G., 1970. The Mathematical Theory of Non-Uniform Gases, vol. 27, The Mathematical Association, ISBN: 0252725484, http://dx.doi.org/10.2307/3611062, URL http://www.jstor.org/stable/3611062?origin=crossref.

Chassagne, Rémi, Bonamy, Cyrille, Chauchat, Julien, 2023. A frictional-collisional model for bedload transport based on kinetic theory of granular flows: Discrete and continuum approaches. J. Fluid Mech. (ISSN: 14697645) 964, 1–39. http://dx.doi.org/10.1017/jfm.2023.335.

Chauchat, Julien, 2018. A comprehensive two-phase flow model for unidirectional sheet-flows. J. Hydraul. Res. (ISSN: 00221686) 56, 15–28. http://dx.doi.org/10.1080/00221686.2017.1289260.

Chialvo, Sebastian, Sun, Jin, Sundaresan, Sankaran, 2012. Bridging the rheology of granular flows in three regimes. Phys. Rev. E (ISSN: 1539-3755) 85 (2), 021305. http://dx.doi.org/10.1103/PhysRevE.85.021305, URL http://link.aps.org/doi/10.1103/PhysRevE.85.021305.

Creyssels, M., Dupont, P., Ould El Moctar, A., Valance, A., Cantat, I., Jenkins, J.T., Pasini, J.M., Rasmussen, K.R., 2009. Saltating particles in a turbulent boundary layer: experiment and theory. J. Fluid Mech. (ISSN: 0022-1120) 625, 47. http://dx.doi.org/10.1017/S0022112008005491, URL http://www.journals.cambridge.org/abstract_S0022112008005491.

Felice, Renzo D.I., 1995. Hydrodynamics of liquid fluidisation. Chem. Eng. Sci. 50, 1213–1245,

Foerster, Samuel F., Louge, Michel Y., Chang, Hongder, Allia, Khedidja, 1994. Measurements of the collision properties of small spheres. Phys. Fluids (ISSN: 10706631) 6 (3), 1108–1115. http://dx.doi.org/10.1063/1.868282, URL http://link.aip.org/link/PHFLE6/v6/i3/p1108/s1&Agg=doi.

Gao, Peng, 2008. Transition between two bed-load transport regimes : Saltation and sheet flow. J. Hydraul. Eng. (ISSN: 0733-9429) 134 (March), 340–349. http://dx.doi.org/10.1061/(ASCE)0733-9429(2008)134:3(340),

Garzó, V., Dufty, J.W., 1999. Dense fluid transport for inelastic hard spheres. Phys. Rev. E (ISSN: 1063-651X) 59 (5), 5895–5911, URL http://www.ncbi.nlm.nih.gov/pubmed/11969571.

Garzó, V., Tenneti, S., Subramaniam, S., Hrenya, C.M., 2012. Enskog kinetic theory for monodisperse gas-solid flows. J. Fluid Mech. (ISSN: 00221120) 712, 129–168. http://dx.doi.org/10.1017/jfm.2012.404.

Gonzalez-Ondina, Jose M., Fraccarollo, Luigi, Liu, Philip L.F., 2018. Two-level, two-phase model for intense, turbulent sediment transport. J. Fluid Mech. (ISSN: 14697645) 839, 198–238. http://dx.doi.org/10.1017/jfm.2017.920.

Hsu, T.-J., Jenkins, J.T., Liu, P. L.-F., 2004. On two-phase sediment transport: sheet flow of massive particles. Proc. R. Soc. A: Math. Phys. Eng. Sci. (ISSN: 1364-5021) 460, 2223–2250. http://dx.doi.org/10.1098/rspa.2003.1273, URL http://rspa.royalsocietypublishing.org/cgi/doi/10.1098/rspa.2003.1273.

Jenkins, James T., 2006. Dense shearing flows of inelastic disks. Phys. Fluids (ISSN: 10706631) 18 (10), 103307. http://dx.doi.org/10.1063/1.2364168, URL http://link.aip.org/link/PHFLE6/v18/i10/p103307/s1&Agg=doi.

Jenkins, James T., 2007. Dense inclined flows of inelastic spheres. Granul. Matter (ISSN: 1434-5021) 10 (1), 47–52. http://dx.doi.org/10.1007/s10035-007-0057-z, URL http://www.springerlink.com/index/10.1007/s10035-007-0057-z.

Jenkins, James T., Berzi, Diego, 2010. Dense inclined flows of inelastic spheres: tests of an extension of kinetic theory. Granul. Matter (ISSN: 1434-5021) 12 (2), 151–158. http://dx.doi.org/10.1007/s10035-010-0169-8, URL http://www.springerlink.com/index/10.1007/s10035-010-0169-8,

Jenkins, J.T., Cantat, I., Valance, A., 2010. Continuum model for steady, fully developed saltation above a horizontal particle bed. Phys. Rev. E 82, 020301. http://dx.doi.org/10.1103/PhysRevE.82.020301, URL http://pre.aps.org/abstract/PRE/v82/i2/e020301.

Jenkins, J.T., Hanes, D.M., 1998. Collisional sheet flows of sediment driven by a turbulent fluid. J. Fluid Mech. 370, 29–52, URL http://journals.cambridge.org/abstract_S0022112098001840.

Jenkins, J.T., Richman, Mark W., 1988. Plane simple shear of smooth inelastic circular disks: the anisotropy of the second moment in the dilute and dense limits. J. Fluid Mech. (ISSN: 0022-1120) 192, 313–328. http://dx.doi.org/10.1017/S0022112088001879, URL http://www.journals.cambridge.org/abstract_S0022112088001879,

Jenkins, J.T., Savage, S.B., 1983. A theory for the rapid flow of identical, smooth, nearly elastic, spherical particles. J. Fluid Mech. 130, 187–202, URL http://journals.cambridge.org/abstract_S0022112083001044.

Jenkins, James T., Zhang, Chao, 2002. Kinetic theory for identical, frictional, nearly elastic spheres. Phys. Fluids (ISSN: 10706631) 14 (3), 1228–1235. http://dx.doi.org/10.1063/1.1449466, URL http://link.aip.org/link/PHFLE6/v14/i3/p1228/s1&Agg=doi.

Komatsu, Teruhisa, Inagaki, Shio, Nakagawa, Naoko, Nasuno, Satoru, 2001. Creep motion in a granular pile exhibiting steady surface flow. Phys. Rev. Lett. (ISSN: 0031-9007) 86 (9), 1757–1760. http://dx.doi.org/10.1103/PhysRevLett.86.1757, URL http://link.aps.org/doi/10.1103/PhysRevLett.86.1757.

Larcher, Michele, Jenkins, James T., 2013. Segregation and mixture profiles in dense, inclined flows of two types of spheres. Phys. Fluids (ISSN: 10706631) 25 (11), 113301. http://dx.doi.org/10.1063/1.4830115, URL http://scitation.aip.org/content/aip/journal/pof2/25/11/10.1063/1.4830115.

Lien, Hui-Pang, Tsai, Fang-Wu, 2003. Sediment concentration distribution of debris flow. J. Hydraul. Eng. (ISSN: 0733-9429) 129 (12), 995–1000. http://dx.doi.org/10.1061/(asce)0733-9429(2003)129:12(995).

McTigue, D.F., 1981. Mixture theory for suspended sediment transport. J. Hydraul. Div. 107 (6), 659–673.

Meyer-Peter, E., Müller, R., 1948. Formulas for Bed-Load Transport. Technical Report, IAHSR.

Mitarai, Namiko, Nakanishi, Hiizu, 2007. Velocity correlations in dense granular shear flows: Effects on energy dissipation and normal stress. Phys. Rev. E (ISSN: 1539-3755) 75 (3), 031305. http://dx.doi.org/10.1103/PhysRevE.75.031305, URL http://link.aps.org/doi/10.1103/PhysRevE.75.031305.

Ni, Wei Jay, Capart, Hervé, 2018. Stresses and drag in turbulent bed load from refractive index-matched experiments. Geophys. Res. Lett. (ISSN: 19448007) 45 (14), 7000–7009. http://dx.doi.org/10.1029/2018GL077571.

Pasini, José Miguel, Jenkins, James T., 2005. Aeolian transport with collisional suspension. Philos. Trans. Ser. A Math. Phys. Eng. Sci. (ISSN: 1364-503X) 363 (1832), 1625–1646. http://dx.doi.org/10.1098/rsta.2005.1598, URL http://www.ncbi.nlm.nih.gov/pubmed/16011936.

Pugh, F.J., Wilson, Kenneth C., 1999. Velocity and concentration distributions in sheet flow above plane beds. J. Hydraul. Eng. 125 (2), 117–125, URL http://link.aip.org/link/?JHEND8/125/117/1.

Ralaiarisoa, J.L., Besnard, J.B., Furieri, B., Dupont, P., Ould El Moctar, A., Naaim-Bouvet, F., Valance, A., 2020. Transition from saltation to collisional regime in windblown sand. Phys. Rev. Lett. (ISSN: 10797114) 124 (19), 198501. http://dx.doi.org/10.1103/PhysRevLett.124.198501, URL https://doi.org/10.1103/PhysRevLett.124.198501.

Revil-Baudard, Thibaud, Chauchat, Julien, Hurther, David, Barraud, Pierre-Alain, 2015. Investigation of sheet-flow processes based on novel acoustic high-resolution velocity and concentration measurements. J. Fluid Mech. (ISSN: 0022-1120) 767, 1–30. http://dx.doi.org/10.1017/jfm.2015.23, URL http://www.journals.cambridge.org/abstract_S0022112015000233.

Richardson, J.F., Zaki, W.N., 1954. The sedimentation of a suspension of uniform spheres under conditions of viscous flow. Chem. Eng. Sci. 3 (2), 65–73.

van Rijn, L.C., 1984. Sediment transport, part I: bed load transport. J. Hydraul. Eng. 110 (10), 1431–1456. http://dx.doi.org/10.1061/(ASCE)0733-9429(1984)110:10(1431), URL http://www.leovanrijn-sediment.com/papers/P2-1984a.pdf.

Rouse, H., 1939. Experiments on the mechanics of sediment suspension. In: Fifth International Congress for Applied Mechanics. John Wiley and Sons, New York, pp. 550–554.

Saha, S., Alam, M., 2016. Normal stress differences , their origin and constitutive relations for a sheared granular fluid. J. Fluid Mech. (ISSN: 14697645) 795, 549–580. http://dx.doi.org/10.1017/jfm.2016.237.

Sauermann, G., Kroy, K., Herrmann, H.J., 2001. A continuum saltation model for sand dunes. Phys. Rev. E 64, 031305. http://dx.doi.org/10.1103/PhysRevE.64.031305, http://arxiv.org/abs/cond-mat/0101377.

Shannon, C.E., 1948. A mathematical theory of communication. Bell Syst. Tech. J. (ISSN: 15387305) 27 (4), 623–656. http://dx.doi.org/10.1002/j.1538-7305.1948.tb00917.x.

Silbert, Leonardo E., 2010. Jamming of frictional spheres and random loose packing. Soft Matter (ISSN: 1744-683X) 6 (13), 2918. http://dx.doi.org/10.1039/c001973a, URL http://xlink.rsc.org/?DOI=c001973a.

Torquato, S., 1995. Nearest-neighbor statistics for packings of hard spheres and disks. Phys. Rev. E 51 (4), 3170–3182, URL http://pre.aps.org/abstract/PRE/v51/i4/p3170_1.

Valance, Alexandre, Berzi, Diego, 2022. Particle saltation over rigid bumpy beds in viscous shearing flows. J. Fluid Mech. (ISSN: 0022-1120) 947, 1–28. http://dx.doi.org/10.1017/jfm.2022.616.

Valance, Alexandre, Rasmussen, Keld Rømer, Ould El Moctar, Ahmed, Dupont, Pascal, 2015. The physics of aeolian sand transport. Comptes Rendus Phys. 16 (1), 105–117. http://dx.doi.org/10.1016/j.crhy.2015.01.006.

Van Driest, E.R., 1956. On turbulent flow near a wall. J. Aeronaut. Sci. 23 (11), 1007–1011. http://dx.doi.org/10.2514/8.3713.

Vescovi, D., Berzi, D., Richard, P., Brodu, N., 2014. Plane shear flows of frictionless spheres: Kinetic theory and 3D soft-sphere discrete element method simulations. Phys. Fluids (ISSN: 1070-6631) 26 (5), 053305. http://dx.doi.org/10.1063/1.4879267, URL http://scitation.aip.org/content/aip/journal/pof2/26/5/10.1063/1.4879267.

Vowinckel, Bernhard, Kempe, Tobias, Fröhlich, Jochen, 2014. Fluid-particle interaction in turbulent open channel flow with fully-resolved mobile beds. Adv. Water Resour. (ISSN: 03091708) 72, 32–44. http://dx.doi.org/10.1016/j.advwatres.2014.04.019, URL http://dx.doi.org/10.1016/j.advwatres.2014.04.019.

Whitaker, Stephen, 1986. Flow in porous media I: A theoretical derivation of Darcy's law. Transp. Porous Media (ISSN: 01693913) 1 (1), 3–25. http://dx.doi.org/10.1007/BF01036523.